Electronic Supplementary Material (ESI) for Journal of Materials Chemistry A.

Supporting information

Two isostructural metal-organic frameworks with unique nickel clusters for $C_2H_2/C_2H_6/C_2H_4$ mixture separation

Hao-Tian Wang, [a] Qiang Chen, [a] Xin Zhang, *[a] Yan-Long Zhao, [a] Ming-Ming Xu, [a] Rui-Biao Lin, [b] Hongliang Huang, [c] Lin-Hua Xie,*[a] Jian-Rong Li [a]

a. *Beijing Key Laboratory for Green Catalysis and Separation and Department of Environmental Chemical Engineering, Faculty of Environment and Life, Beijing University of Technology, Beijing 100124, China*
b. *MOE Key Laboratory of Bioinorganic and Synthetic Chemistry, School of Chemistry, Sun Yat-Sen University, Guangzhou, 510006, China*
c. *State Key Laboratory of Separation Membranes and Membrane Processes, School of Chemistry and Chemical Engineering, Tiangong University, Tianjin 300387, China.*

**correspondence: zhang.xin@bjut.edu.cn, xielinhua@bjut.edu.cn*

Synthesis and Characterization of the Ligands

All chemicals and solvents were purchased and used as received unless specified. The synthesis of ligands is summarized in Scheme S1 and Scheme S2. And the $^{1}H/^{13}C$ NMR spectra of two ligands are showed in Figure S1-4.

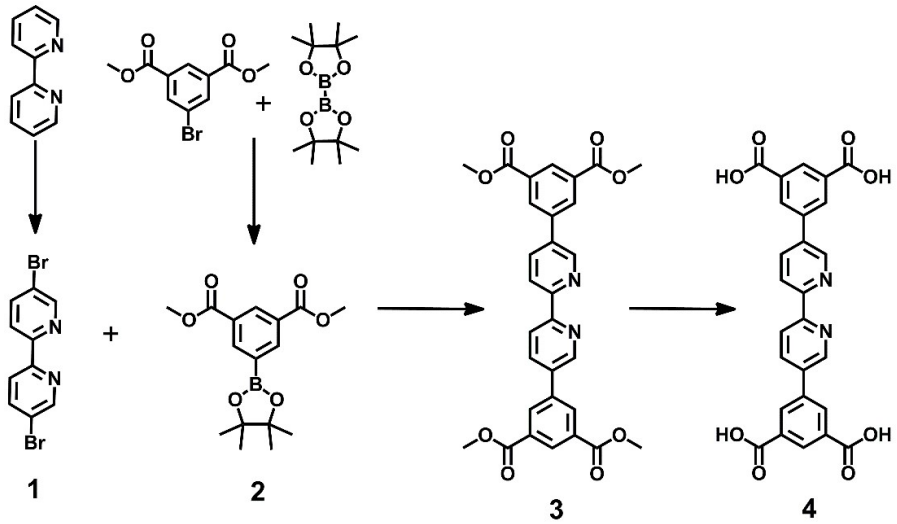

Scheme S1. Synthetic route for H_4DiBP.

Synthesis of 5,5'-dibromo-2,2'-bipyridine (1).

This compound was synthesized following a modified literature procedure[1]. 2,2´-Bipyridine (20 g, 130 mmol) was dissolved in 80 mL of methanol before 39 mL of 40 % HBr (aq.) was added dropwisely to the solution. After overnight reaction at room temperature, the solvent was removed by rotary evaporation, and the resulting residue was dried at 120 °C for 12 h to yield 2,2´-bipyridine hydrobromide (95 %). 2,2´-Bipyridine hydrobromide (24 g, 75.4 mmol) and bromine (40 g, 125 mmol) were combined in a Teflon-lined stainless-steel Parr bomb and heated at 180 °C for 96 h. After cooling down to room temperature, the crude product was recrystallized in N, N´-dimethylformamide (DMF), and neutralized with aqueous KOH solution to obtain pure 5,5´-dibromo-2,2´-bipyridine. The product was further purified by a flash silica gel column using chloroform as the eluent (yield: 40 %). ^{1}H NMR ($CDCl_3$, 400 MHz): 8.73 (s, 1 H); 8.31 (d, 1 H); 7.96 (dd, 1 H).

Synthesis of dimethyl 5-(4,4,5,5-tetramethyl-1,3,2-dioxaborolan-2-yl)isophthalate (2).

This compound was synthesized following a modified literature procedure[2]. Dimethyl 5-bromoisophthalate (25 g, 91.5 mmol), bis(pinacolato)diborane (28 g, 110 mmol), potassium acetate (26 g, 264.9 mmol) and $Pd(dppf)_2Cl_2$ (1 g, 1.4 mmol) were added into a double necked round bottom flask with a magnetic stir bar. After the air was removed by vacuum and the flask was refilled with nitrogen for three times, 150 mL of degassed dioxane (bubbled with nitrogen for 30 minutes) was added through cannula transfer. Then the reaction was heated at 100 °C overnight and afterward cooled down to room temperature, extracted with ethyl acetate (20 mL). The organic layer was dried with Na_2SO_4 and the solvent was removed by a rotavapor. The crude product was purified by column chromatography (silica gel, ethyl acetate/petroleum ether, 6 v%). Yield 69.3%. ^{1}H NMR ($CDCl_3$, 400 MHz): 8.79 (s, 1 H); 8.63 (d, 2 H); 3.97 (s, 6 H) 1.39 (s, 12 H).

Synthesis of tetramethyl 5,5'-([2,2'-bipyridine]-5,5'-diyl)diisophthalate (3).

The compound **1** (2.512 g, 8 mmol) and **2** (7.68 g, 24 mmol) with potassium phosphate (5.28 g, 24.9 mmol) and $Pd(PPh_3)_4$ (0.628 g, 0.543 mmol) were added into a double necked round bottom flask with a magnetic stir bar. After the air was removed by vacuum and the flask was refilled with nitrogen for three times, 150 mL of degassed dioxane (bubbled with nitrogen for 30 minutes) was added through cannula transfer. The resulting mixture was heated at 110 °C for three days with magnetic stirring. After cooled down to room temperature, the crude product was filtered through silica gel and washed with MeOH/CH_2Cl_2 (1/1). After the solvent of filtrate was evaporated, the solid was recrystallized from ethanol to obtain a light-yellow solid in 70% yield. ^{1}H NMR ($CDCl_3$, 400 MHz): 9.04 (d, 1 H); 8.76 (d, 1 H); 8.64 (d, 1 H); 8.57 (d, 2 H); 8.15 (dd, 1 H); 3.95 (s, 6 H).

Synthesis of 5,5'-([2,2'-bipyridine]-5,5'-diyl)diisophthalic acid (H_4DiBP) (4).

Compound **3** (10 g, 20 mmol) and NaOH (4 g, 100 mmol) were added to the mixed solvent of THF/MeOH/H_2O (1: 1: 1). The mixture was stirred under reflux overnight and the organic solvents were removed under a vacuum. 1M HCl was added dropwisely to the remaining aqueous solution until the solution was at pH = 7. The solid was collected by filtration, washed with water and dried to yield H_4DiBP, 90% yield. ^{1}H NMR (d6-DMSO, 400 MHz): 9.11(d, 2 H); 8.57 (d, 2 H); 8.54 (s, 2 H); 8.49 (d, 4 H) 8.37 (dd, 2 H). ^{13}C NMR (d6-DMSO): δ 121.27, 130.04, 131.84, 133.07, 134.78, 136.26, 138.14, 148.11, 154.84 and 166.92. (Figure S1-S2).

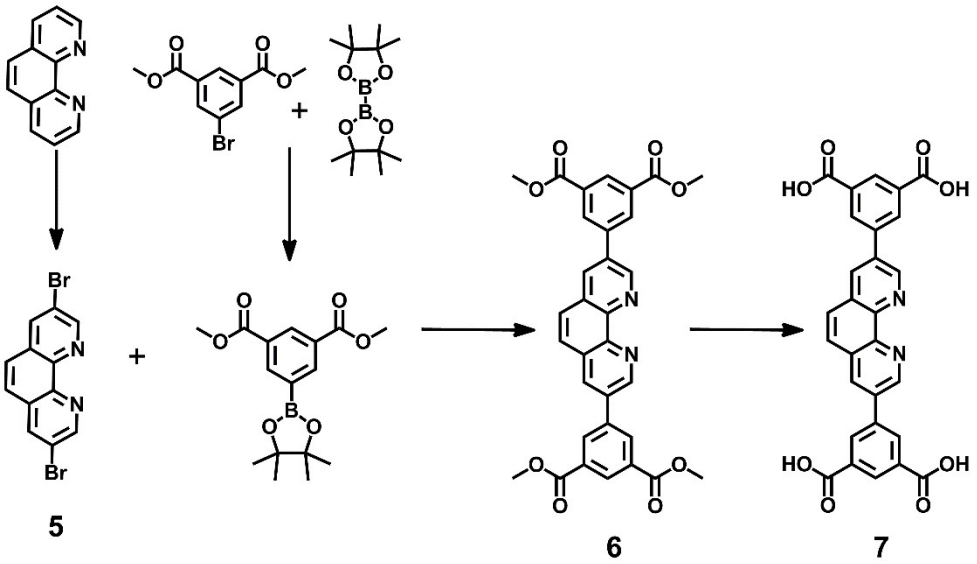

Scheme S2. Synthetic route for H_4Diphen.

Synthesis of 3,8-dibromo-1,10-phenanthroline (5).

This compound was synthesized following a modified literature procedure[3]. In a 1000 mL three-necked round-bottomed flask, a mixture of 1,10-phenanthroline (10g, 55.6 mmol), S_2Cl_2 (16 mL), pyridine (15 mL), and 1-chlorobutane (400 mL) was heated to 100 °C, then Br_2 (10.5 mL) was added very slowly. The reaction mixture was refluxed at 100 °C for 12 h. After cooled down to room temperature, the reaction was quenched by adding about 20 mL saturated NaOH (aq). After the solvent was evaporated, the crude solid product was washed with water and extracted with CH_2Cl_2. After the solvent was evaporated, the solid was washed with petroleum ether, and dissolved with CH_2Cl_2. The solution was filtered through silica gel and CH_2Cl_2 was removed with a rotavapor to afford pure product (12 g; 35 mmol; 63 %). ^{1}HNMR (400 MHz, $CDCl_3$): 9.21 (d, 1H), 8.43 (d, 1H), 7.78 (d, 1H).

Synthesis of 5,5'-(1,10-phenanthroline-3,8-diyl)diisophthalate (6).

The synthesis method is the same as **compound 3** synthesis, except that compound **1** was replaced by compound **5**. The solid was recrystallized from ethanol and dried to obtain a

bright yellow solid in 70% yield. ^{1}HNMR (400 MHz, d6-DMSO): 9.52 (d, 1H), 8.81 (s, 1H), 8.68 (s, 2H), 8.55 (d, 1H), 8.00 (s, 1H), 4.06 (s, 6H).

Synthesis of 5,5'-(1,10-phenanthroline-3,8-diyl)diisophthalic acid (H_4DiPhen) (7).
The synthesis method is the same as **compound 4** synthesis, except that compound **3** was replaced by compound **6**. The solid was collected by filtration, washed with water and dried to yield H_4DiPhen, 90% yield. ^{1}H NMR (d6-DMSO, 400 MHz): 9.55 (d, 2 H); 9.32 (d, 2 H); 8.65 (d, 4 H); 8.53 (s, 2 H) 8.33 (s, 2 H). ^{13}C NMR (d6-DMSO): δ 128.01, 129.08, 130.18, 131.94, 133.71, 133.76, 134.45, 137.96, 145.15, 148.91 and 167.16. (Figure S3,4).

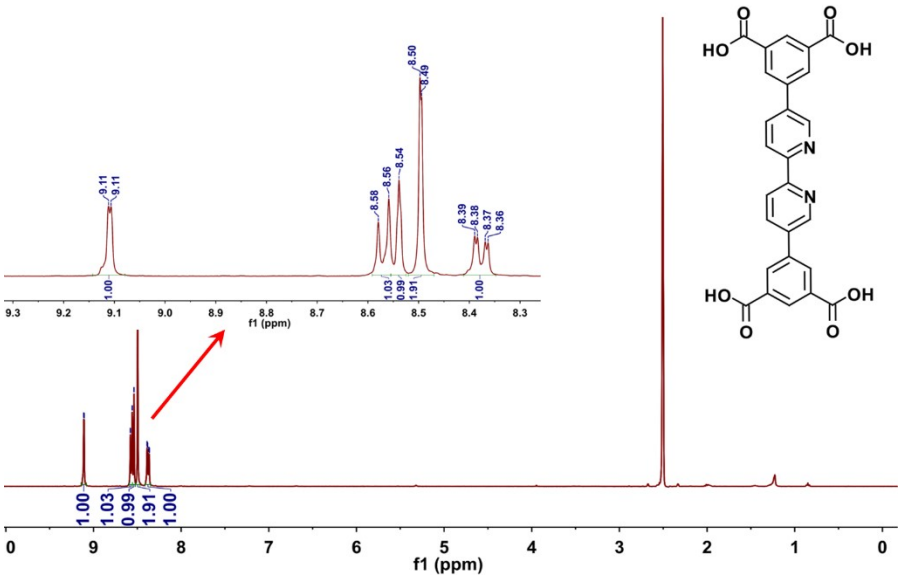

Figure S1. ^{1}H NMR spectra of compound **4.**

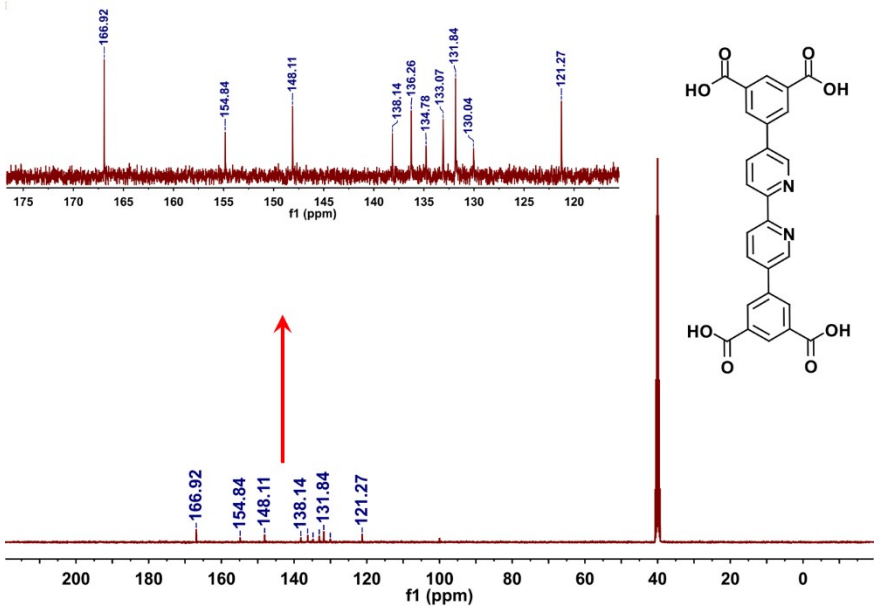

Figure S2. ^{13}C NMR spectra of compound **4.**

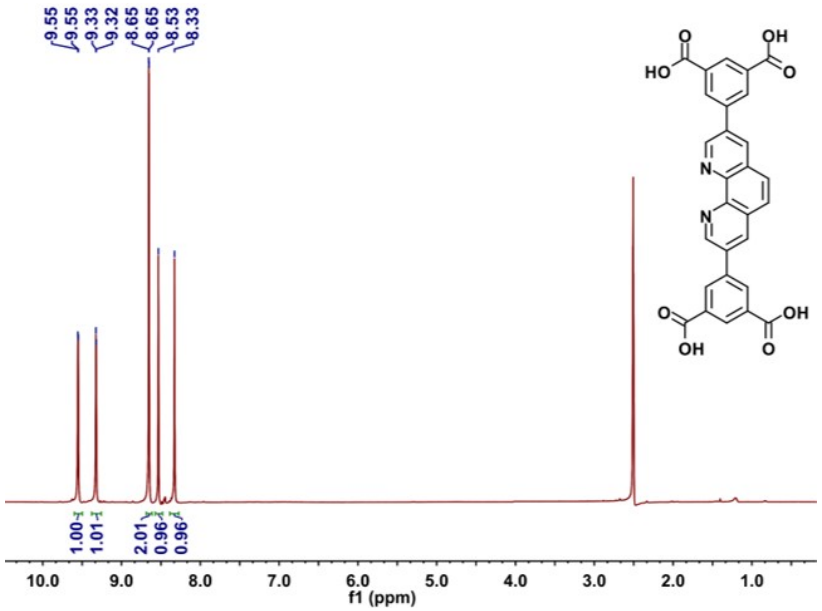

Figure S3. ^{1}H NMR spectra of compound **7.**

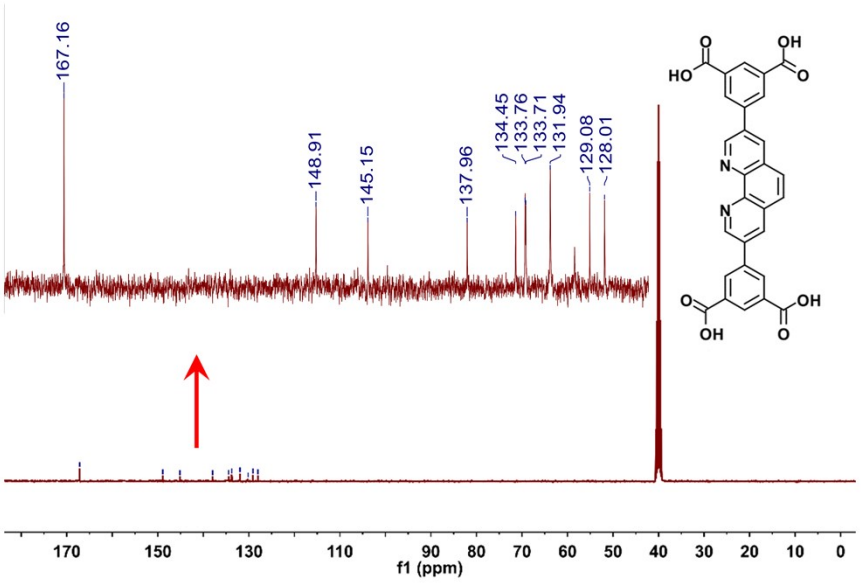

Figure S4. ^{13}C NMR spectra of compound **7.**

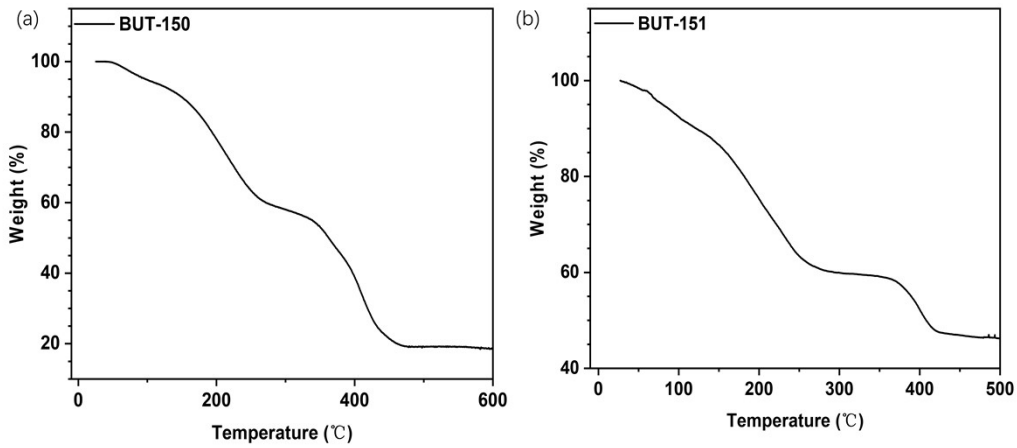

Figure S5. TGA curves of fresh MOF samples (a) BUT-150 and (b) BUT-151.

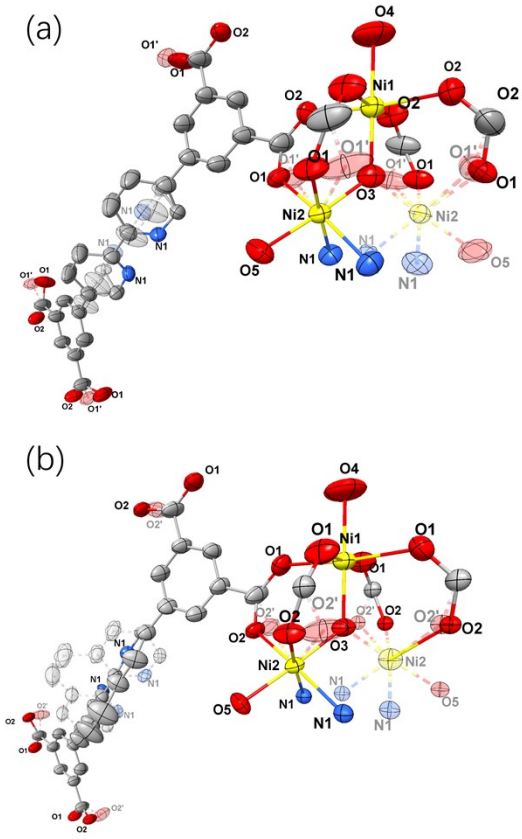

Figure S6. An ORTEP view of building units of BUT-150 (a) and BUT-151 (b). Displacement ellipsoids are represented by 50% probability level. One part of the disordered model is shown in transparency for clarity

Table S1. Crystal data and structure refinement for BUT-150 and BUT-151.

Identification code	BUT-150	BUT-151
CCDC	2142458	2142608
Molecular formula	$Ni_2(\mu_2\text{-}OH_2)(DiBP)\cdot(H_2O)_2\cdot(DMA)_{4.5}$	$Ni_2(\mu_2\text{-}OH_2)(DiPhen)\cdot(H_2O)_2\cdot(DMA)_{4.5}$
Formula weight	1043.89	1067.91
Temperature/K	271(2)	220(2)
Crystal system	cubic	cubic
Space group	Fd-3m	Fd-3m
a/Å	40.5215(5)	40.5322(3)
Volume/Å^3	66536(2)	66588.7(15)
Z	48	48
ρ_{calc}g/cm^3	1.251	1.278
μ/mm^{-1}	1.396	0.745
F(000)	26304	26880
Crystal size/mm^3	0.15× 0.15× 0.15	0.15× 0.15× 0.15
Radiation	Cu Kα (λ = 1.54178)	Mo Kα (λ = 0.71073)
2θ range for data collection/°	3.779 to 68.141	3.482 to 29.379
Index ranges	-45<=h<=48, -48<=k<=48, -39<=l<=39	-30<=h<=42, -33<=k<=51, -48<=l<=11
Reflections collected	37719	18945
Independent reflections	2759 [R(int) = 0.0853]	3882 [R(int) = 0.0375]
Data/restraints/parameters	2759 / 139 / 139	3882 / 0 / 148
Goodness-of-fit on F^2	1.013	1.017
Final R indexes [I>=2σ (I)]	R_1 = 0.0857, wR_2 = 0.2057	R_1 = 0.0806, wR_2 = 0.2212
Final R indexes [all data]	R_1 = 0.1037, wR_2 = 0.2175	R_1 = 0.0971, wR_2 = 0.2319
Largest diff. peak/hole / e Å^{-3}	0.941 and -0.424	0.547 and -0.379

$R_1 = \Sigma||F_o| - |F_c||/\Sigma|F_o|$; $wR_2 = |\Sigma w(|F_o|^2 - |F_c|^2)|/\Sigma|w(F_o)^2|^{1/2}$, where $w = 1/[\sigma^2(F_o^2) + (aP)^2 + bP]$. $P = (F_o^2 + 2F_c^2)/3$

Isosteric heat of adsorption calculation.

A Virial equation comprising of the temperature-independent parameters a_i and b_i was employed to calculate the enthalpies of adsorption for C_2H_6, C_2H_4 and C_2H_2 in BUT-150 and BUT-151, which measured at different temperatures 273K and 298 K.

$$\ln(p) = \ln(N) + \left(\frac{1}{T}\right)\sum_{i=0}^{m} a_i \times N^i + \sum_{j=0}^{n} b_j \times N^j \qquad (1)$$

$$Q_{st} = -R \times \sum_{i=0}^{m} a_i \times N^i \quad (2)$$

where P is the pressure (mmHg), N is the adsorbed quantity (mg/g), T is the temperature (K), R is the gas constant (8.314 J/(K·mol), a_i and b_i are virial coefficients.

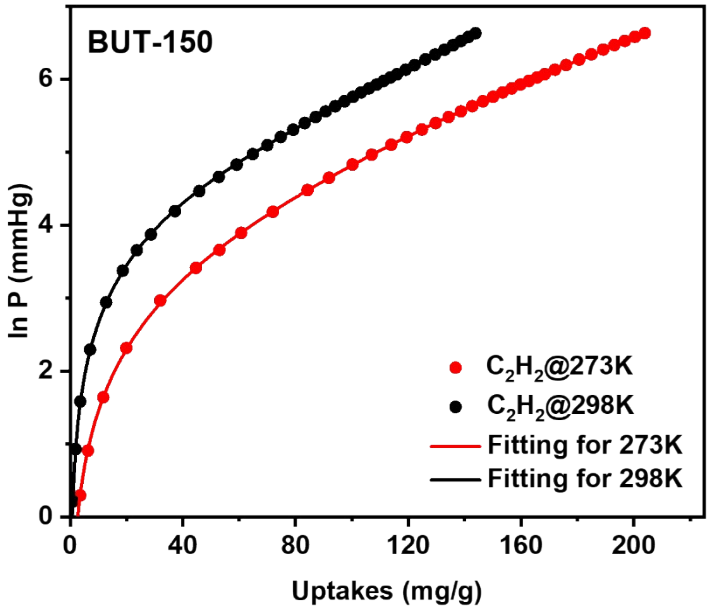

Equation	y=ln(x)+1/K*(a0+a1*x+a2*x^2+a3*x^3+a4*x^4+a5*x^5)+(b0+b1*x+b2*x^2)	
a0*	-4153.23066 ± 19.58928	-4153.23066 ± 19.58928
a1*	23.64694 ± 0.66049	23.64694 ± 0.66049
a2*	-0.1541 ± 0.0062	-0.1541 ± 0.0062
a3*	5.09079E-4 ± 7.03356E-5	5.09079E-4 ± 7.03356E-5
a4*	-2.30916E-6 ± 3.92608E-7	-2.30916E-6 ± 3.92608E-7
a5*	3.94461E-9 ± 7.78282E-10	3.94461E-9 ± 7.78282E-10
b0*	14.17468 ± 0.06815	14.17468 ± 0.06815
b1*	-0.06638 ± 0.0023	-0.06638 ± 0.0023
b2*	3.70976E-4 ± 1.56229E-5	3.70976E-4 ± 1.56229E-5
K	273 ± 0	298 ± 0
Reduced Chi-Sqr*	1.02217E-4	
R-Square (COD)	0.99997	0.99998
R-Square (COD)*	0.99998	
Adj. R-Square*	0.99998	

Figure S7. Virial fitting of the C_2H_2 adsorption isotherms at 273 K and 298 K for BUT-150 for Qst calculation.

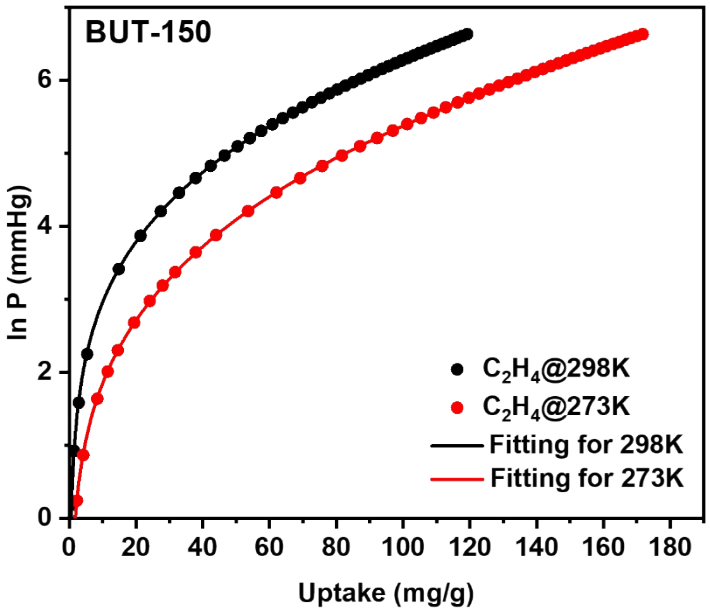

Equation	y=ln(x)+1/K*(a0+a1*x+a2*x^2+a3*x^3+a4*x^4+a5*x^5)+(b0+b1*x+b2*x^2)	
a0*	-3735.38775 ± 16.81156	-3735.38775 ± 16.81156
a1*	12.07952 ± 0.66852	12.07952 ± 0.66852
a2*	-0.02233 ± 0.00713	-0.02233 ± 0.00713
a3*	-4.19129E-4 ± 9.67455E-5	-4.19129E-4 ± 9.67455E-5
a4*	3.00863E-6 ± 6.40201E-7	3.00863E-6 ± 6.40201E-7
a5*	-6.97785E-9 ± 1.50104E-9	-6.97785E-9 ± 1.50104E-9
b0*	13.06548 ± 0.05861	13.06548 ± 0.05861
b1*	-0.02786 ± 0.00233	-0.02786 ± 0.00233
b2*	1.25624E-4 ± 1.88036E-5	1.25624E-4 ± 1.88036E-5
K	298 ± 0	273 ± 0
Reduced Chi-Sqr*	8.07331E-5	
R-Square (COD)	0.99997	0.99999
R-Square (COD)*	0.99998	
Adj. R-Square*	0.99998	

Figure S8. Virial fitting of the C_2H_4 adsorption isotherms at 273 K and 298 K for BUT-150 for Qst calculation.

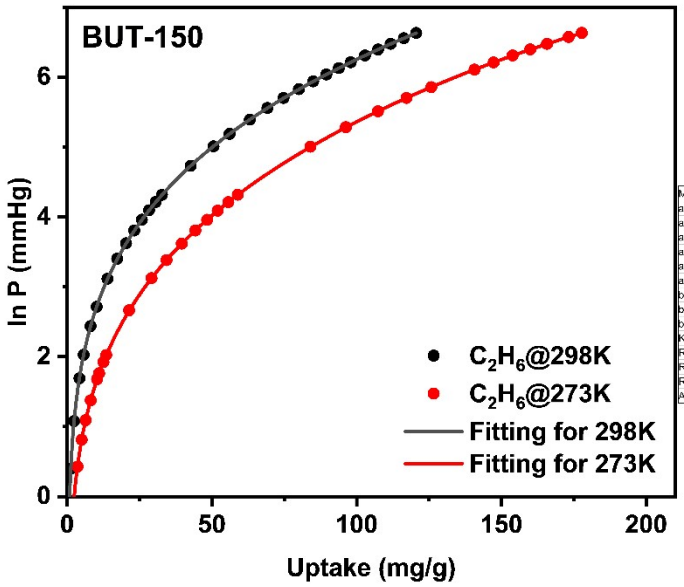

Model	Qst (User)	
a0*	-3549.37421 ± 9.06155	-3549.37421 ± 9.06155
a1*	10.10568 ± 0.43061	10.10568 ± 0.43061
a2*	-0.0698 ± 0.00474	-0.0698 ± 0.00474
a3*	5.07398E-4 ± 5.64733E-5	5.07398E-4 ± 5.64733E-5
a4*	-2.14596E-6 ± 3.72312E-7	-2.14596E-6 ± 3.72312E-7
a5*	3.59337E-9 ± 8.66516E-10	3.59337E-9 ± 8.66516E-10
b0*	12.05945 ± 0.03168	12.05945 ± 0.03168
b1*	-0.0074 ± 0.00149	-0.0074 ± 0.00149
b2*	8.92317E-6 ± 1.25638E-5	8.92317E-6 ± 1.25638E-5
K	298 ± 0	273 ± 0
Reduced Chi-Sqr*	2.76701E-5	
R-Square (COD)	0.99999	1
R-Square (COD)*	1	
Adj. R-Square^	0.99999	

Figure S9. Virial fitting of the C_2H_6 adsorption isotherms at 273 K and 298 K for BUT-150 for Qst calculation.

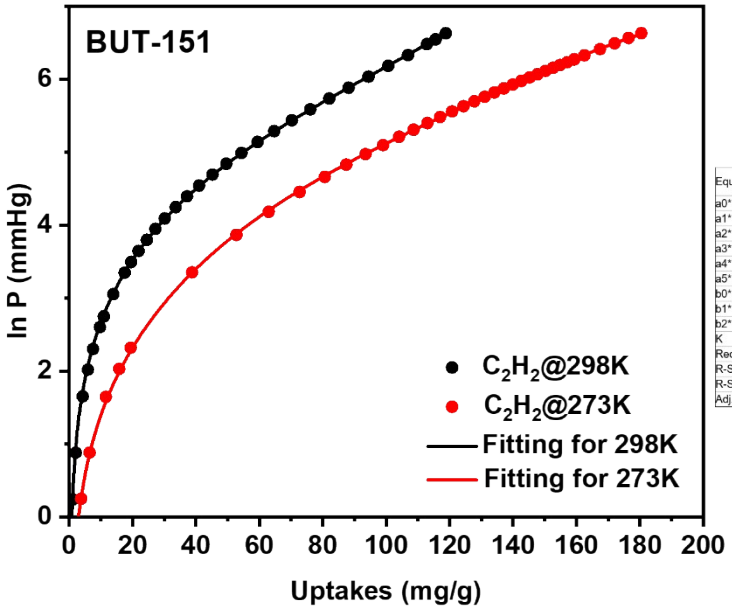

Equation	y=ln(x)+1/K*(a0+a1*x+a2*x^2+a3*x^3+a4*x^4+a5*x^5)+(b0+b1*x+b2*x^2)	
a0*	-4433.8448 ± 85.75659	-4433.8448 ± 85.75659
a1*	29.9447 ± 4.33881	29.9447 ± 4.33881
a2*	-0.21334 ± 0.04478	-0.21334 ± 0.04478
a3*	1.12437E-4 ± 4.48102E-4	1.12437E-4 ± 4.48102E-4
a4*	6.46893E-7 ± 2.89902E-6	6.46893E-7 ± 2.89902E-6
a5*	-2.87425E-9 ± 6.61869E-9	-2.87425E-9 ± 6.61869E-9
b0*	15.06798 ± 0.29641	15.06798 ± 0.29641
b1*	-0.08179 ± 0.0148	-0.08179 ± 0.0148
b2*	6.17056E-4 ± 1.26477E-4	6.17056E-4 ± 1.26477E-4
K	298 ± 0	273 ± 0
Reduced Chi-Sqr*	0.00255	
R-Square (COD)	0.99937	0.99993
R-Square (COD)*	0.99965	
Adj. R-Square*	0.99961	

Figure S10. Virial fitting of the C_2H_2 adsorption isotherms at 273 K and 298 K for BUT-151 for Qst calculation.

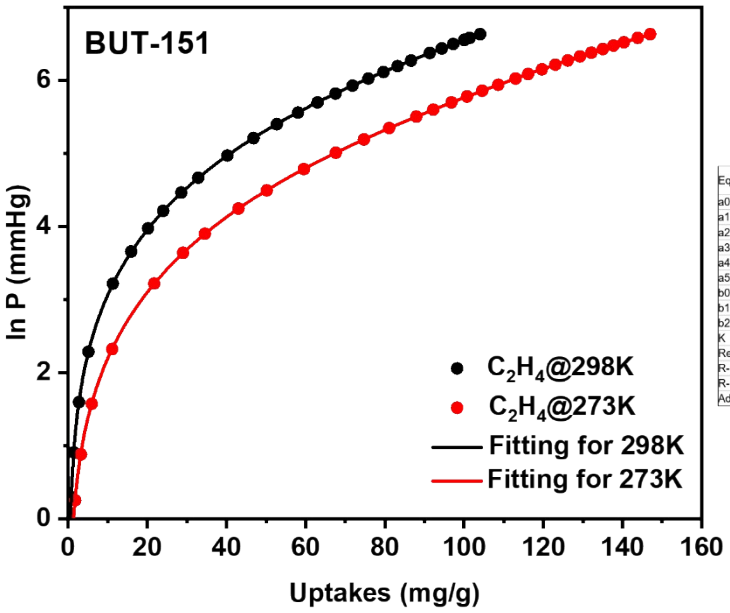

Equation	y=ln(x)+1/K*(a0+a1*x+a2*x^2+a3*x^3+a4*x^4+a5*x^5)+(b0+b1*x+b2*x^2)	
a0*	-2882.04572 ± 16.11991	-2882.04572 ± 16.11991
a1*	5.94041 ± 0.80248	5.94041 ± 0.80248
a2*	-0.06562 ± 0.01043	-0.06562 ± 0.01043
a3*	5.55374E-4 ± 1.68262E-4	5.55374E-4 ± 1.68262E-4
a4*	-2.03359E-6 ± 1.30781E-6	-2.03359E-6 ± 1.30781E-6
a5*	2.5731E-9 ± 3.59992E-9	2.5731E-9 ± 3.59992E-9
b0*	10.19291 ± 0.05699	10.19291 ± 0.05699
b1*	0.00611 ± 0.00287	0.00611 ± 0.00287
b2*	-2.4491E-5 ± 2.71162E-5	-2.4491E-5 ± 2.71162E-5
K	298 ± 0	273 ± 0
Reduced Chi-Sqr*	7.03267E-5	
R-Square (COD)	1	0.99998
R-Square (COD)*	0.99999	
Adj. R-Square*	0.99999	

Figure S11. Virial fitting of the C_2H_4 adsorption isotherms at 273 K and 298 K for BUT-151 for Qst calculation.

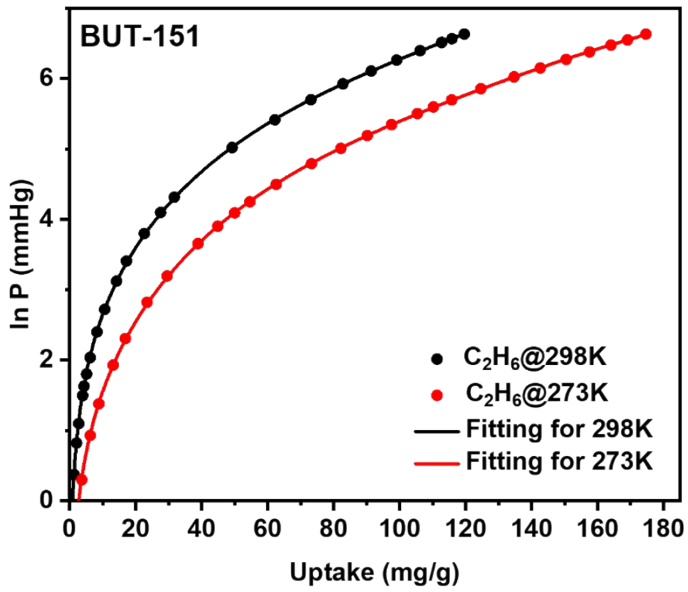

Equation	y=ln(x)+1/K*(a0+a1*x+a2*x^2+a3*x^3+a4*x^4+a5*x^5)+(b0+b1*x+b2*x^2)	
a0*	-3743.82805 ± 50.92524	-3743.82805 ± 50.92524
a1*	18.66328 ± 2.65173	18.66328 ± 2.65173
a2*	-0.14242 ± 0.03008	-0.14242 ± 0.03008
a3*	5.49919E-4 ± 3.27809E-4	5.49919E-4 ± 3.27809E-4
a4*	-1.20396E-6 ± 2.20397E-6	-1.20396E-6 ± 2.20397E-6
a5*	2.94858E-10 ± 5.23493E-9	2.94858E-10 ± 5.23493E-9
b0*	12.59451 ± 0.17379	12.59451 ± 0.17379
b1*	-0.0284 ± 0.00891	-0.0284 ± 0.00891
b2*	1.54469E-4 ± 7.56394E-5	1.54469E-4 ± 7.56394E-5
K	298 ± 0	273 ± 0
Reduced Chi-Sqr*	8.32478E-4	
R-Square (COD)	0.99987	0.99994
R-Square (COD)*	0.9999	
Adj. R-Square*	0.99988	

Figure S12. Virial fitting of the C_2H_6 adsorption isotherms at 273 K and 298 K for BUT-151 for Qst calculation.

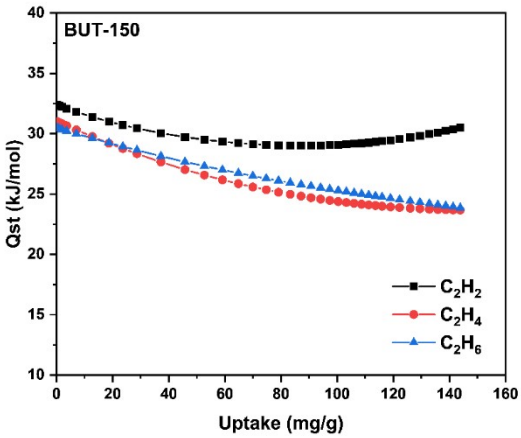

Figure S13. Isosteric heats of adsorption of C_2H_2, C_2H_4 and C_2H_6 for BUT-150 calculated using Virial method with adsorption isotherms at 273 and 298 K.

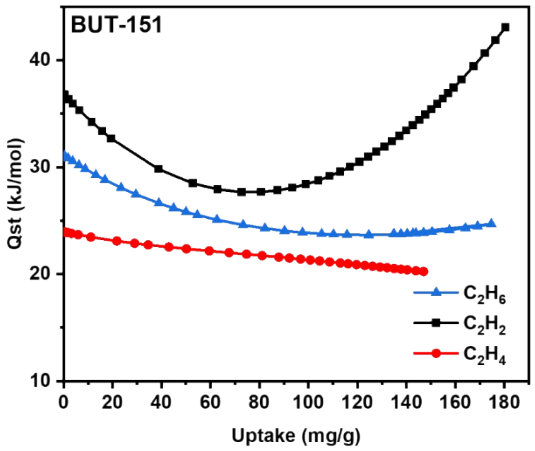

Figure S14. Isosteric heats of adsorption of C_2H_2, C_2H_4 and C_2H_6 on BUT-151 calculated using Virial method with adsorption isotherms at 273 and 298 K.

Calculation of selectivity via ideal adsorption solution theory (IAST).

It was used to estimate the composition of the adsorbed phase from the data of single component isotherms and predict the selectivities of binary mixtures C_2H_2/C_2H_4 and C_2H_6/C_2H_4. IAST calculations of C_2H_2/C_2H_4 (50/50, v/v,) and C_2H_6/C_2H_4 (50/50, v/v) mixtures were performed by:

$$S_{ads} = \frac{q_1/q_2}{p_1/p_2} \qquad (3)$$

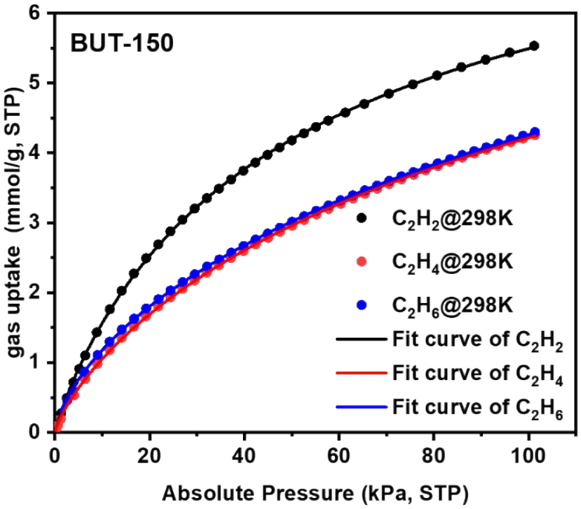

Equation	A1*b1*x^c1/[1+b1*x^c1]		
A1	8.47685 ± 0.07165	10.0569 ± 0.20695	12.989 ± 0.33485
b1	0.02782 ± 2.58133E-4	0.01892 ± 1.86743E-4	0.02049 ± 3.39893E-4
c1	0.91042 ± 0.00594	0.79095 ± 0.00623	0.68851 ± 0.00488
Reduced Chi-Sqr	2.2408E-4	1.64802E-4	1.08733E-4
R-Square (COD)	0.99994	0.99991	0.99992
Adj. R-Square	0.99993	0.99991	0.99991

Figure S15. Adsorption isotherms of BUT-150 at 298 K and fitting parameters by single-site Langmuir-Freundlich model.

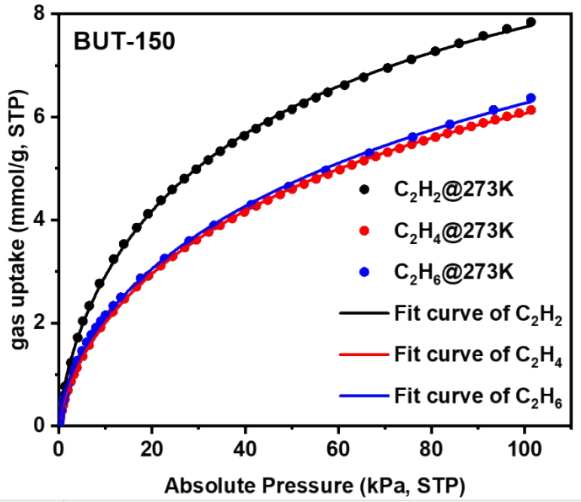

Equation	A1*b1*x^c1/[1+b1*x^c1]		
A1	12.7884 ± 0.25849	12.18664 ± 0.23649	15.59108 ± 0.94639
b1	0.05678 ± 7.77742E-4	0.03903 ± 4.64655E-4	0.03678 ± 0.00171
c1	0.71604 ± 0.00992	0.70251 ± 0.00662	0.6308 ± 0.01202
Reduced Chi-Sqr	0.00184	6.46947E-4	0.00172
R-Square (COD)	0.99972	0.99985	0.99961
Adj. R-Square	0.9997	0.99984	0.99958

Figure S16. Adsorption isotherms of BUT-150 at 273 K and fitting parameters by single-site Langmuir-Freundlich model.

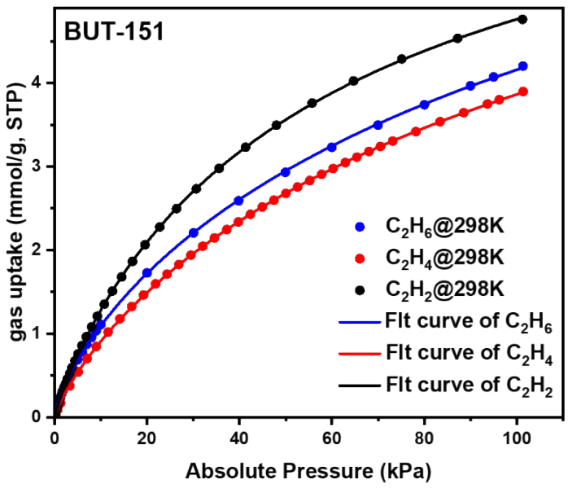

Equation	A1*b1*x^c1/[1+b1*x^c1]		
A1	11.29563 ± 0.43434	9.31273 ± 0.23907	7.69915 ± 0.03559
b1	0.01928 ± 5.63016E-4	0.0181 ± 2.63413E-4	0.03142 ± 9.48987E-5
c1	0.72265 ± 0.007	0.77893 ± 0.00666	0.832 ± 0.0022
Reduced Chi-Sqr	1.73863E-4	1.01994E-4	2.74203E-5
R-Square (COD)	0.99992	0.99994	0.99999
Adj. R-Square	0.99991	0.99994	0.99999

Figure S17. Adsorption isotherms of BUT-151 at 298 K and fitting parameters by single-site Langmuir-Freundlich model.

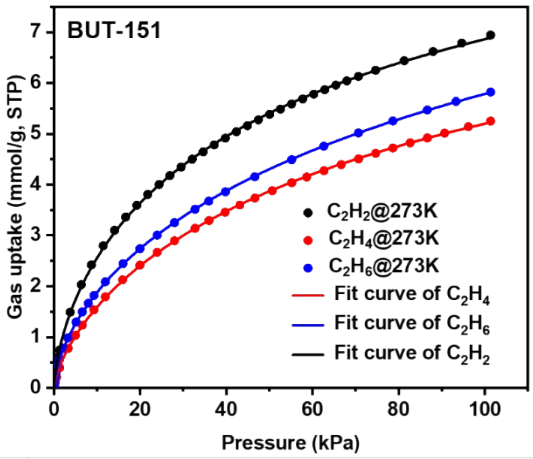

Equation	A1*b1*x^c1/[1+b1*x^c1]		
A1	10.97865 ± 0.23909	12.50099 ± 0.27624	14.93543 ± 0.39055
b1	0.03193 ± 3.98599E-4	0.05427 ± 7.55948E-4	0.03273 ± 6.35699E-4
c1	0.7248 ± 0.00705	0.67524 ± 0.00859	0.64293 ± 0.00521
Reduced Chi-Sqr	2.93964E-4	0.00103	2.59104E-4
R-Square (COD)	0.99992	0.99981	0.99994
Adj. R-Square	0.99991	0.9998	0.99993

Figure S18. Adsorption isotherms of BUT-151 at 273 K and fitting parameters by single-site Langmuir-Freundlich model.

DFT Computational Details.

DFT calculations were carried out using the CP2K code.[4] All calculations employed a mixed Gaussian and planewave basis sets. Core electrons were represented with norm-conserving Goedecker-Teter-Hutter pseudopotentials,[5-7] and the valence electron wavefunction was expanded in a triplet-zeta basis set with polarization functions[8] along

with an auxiliary plane wave basis set with an energy cutoff of 360 eV. The generalized gradient approximation exchange-correlation functional of Perdew, Burke, and Enzerhof (PBE)[9] was used. Each configuration was optimized with the Broyden-Fletcher-Goldfarb-Shanno (BGFS) algorithm with SCF convergence criteria of 1.0×10^{-8} au. To compensate the long-range van der Waals dispersion interaction between the adsorbate and the zeolite, the DFT-D3 scheme[10] with an empirical damped potential term was added into the energies obtained from exchange-correlation functional in all calculations.

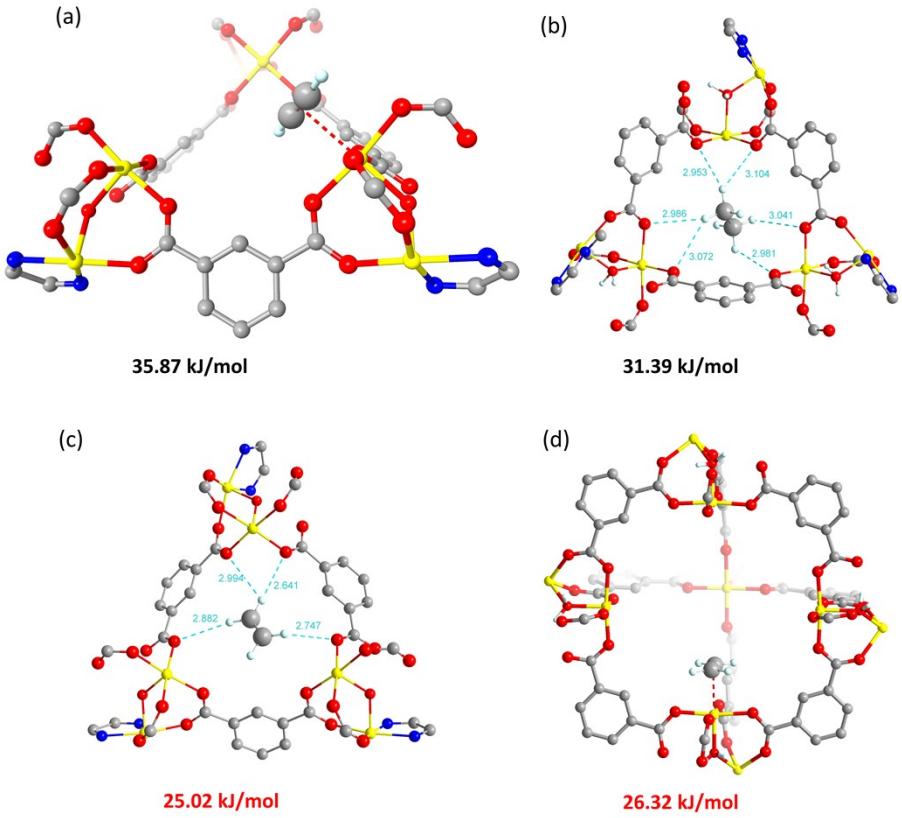

Figure S19. The preferential adsorption sites and corresponding adsorption energies of (a) C_2H_2, (b) C_2H_6 and (c,d) C_2H_4 determined by DFT calculation.

Kinetic Selectivity and Equilibrium Uptake of Acetylene Ethylene and Ethane.

The adsorption kinetics were measured on a MicrotracBEL BELSORP-Max II adsorption equipment at 273 K. The as-synthesized samples (about 200 mg) were degasified through dynamic vacuuming at 393 K for 6 h before the measurements.

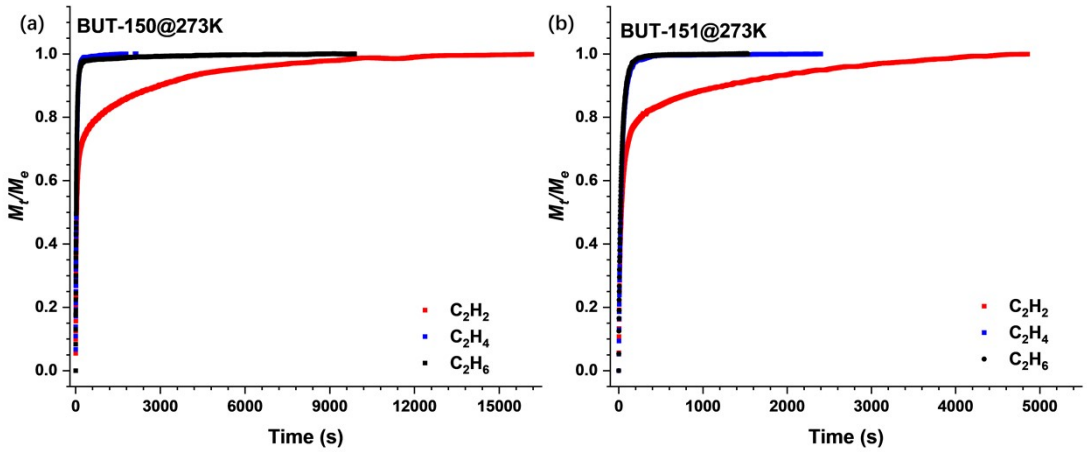

Figure S20. (a) BUT-150 and (b) BUT-151 kinetic uptake plots of ethylene (blue), ethane (black) and acetylene (red) at 273 K.

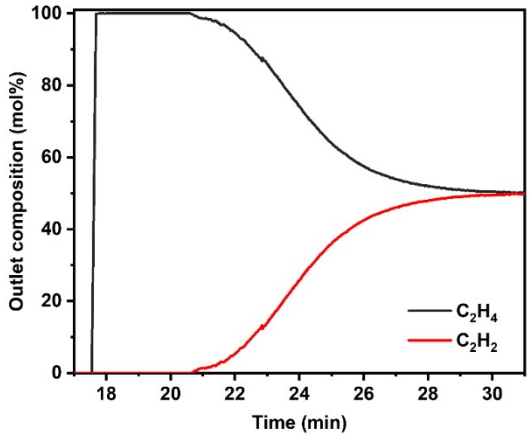

Figure S21. Breakthrough curve of BUT-150 for the separation of 1:1 (v/v) C_2H_2/C_2H_4 gas mixture at 298 K and 1 atm, where the flow rate of the mixed gas is 2 mL/min.

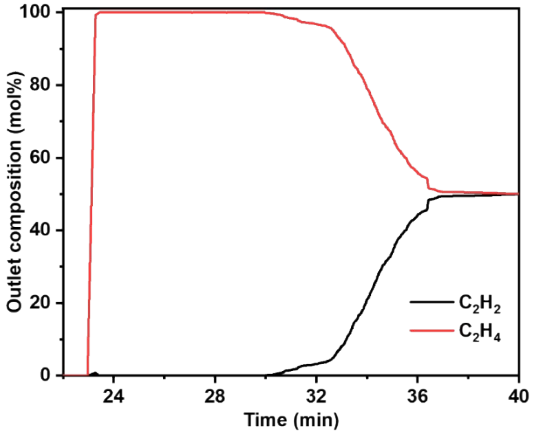

Figure S22. Breakthrough curve of BUT-151 for the separation of 1:1 (v/v) C_2H_2/C_2H_4 gas mixture at 298 K and 1 atm, where the flow rate of the mixed gas is 2 mL/min.

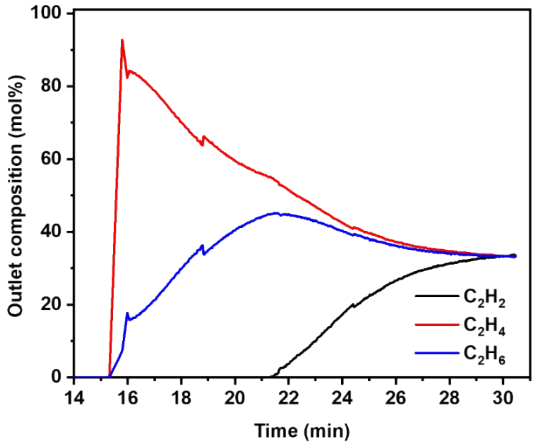

Figure S23. Breakthrough curve of BUT-150 for the separation of a ternary 1:1:1 (v/v/v) $C_2H_2/C_2H_4/C_2H_6$ gas mixture at 298 K and 1 atm, where the flow rate of the mixed gas is 2 mL/min.

Table S2. The adsorption capacity and separation selectivity of C_2H_2 and C_2H_6 selective materials at room temperature and 1 bar.

MOF	C_2H_6 uptake (mmol/g)	C_2H_2 uptake (mmol/g)	C_2H_6/C_2H_4 (1/1, v/v)	C_2H_2/C_2H_4 (1/1, v/v)	Ref.
BUT-150	4.30	5.53	1.15	1.82	This work
BUT-151	3.99	4.8	1.26	1.61	This work
BUT-150※	6.38	7.84	1.13	1.97	This work
BUT-151※	5.82	6.02	1.36	2.31	This work
TJT-100	3.75	4.46	1.8*	1.2*	11
TJT-100※	4.38	5.7	3*	3.8*	11
Azole-Th-1	4.47	3.62	1.46	1.0	12
ZJNU-115	4.20	4.73	1.56	2.05*	13
ZJNU-7	4.13	5.04	1.56	1.77	14
Ag-PCM102‡	3.69	4.59	--	1.5	15
UPC-612	3.57	3.01	1.4	1.08	16
UPC-613	2.54	2.83	1.45	1.39	16
MOF-525	2.70	2.64	1.25	1.44	16
MOF-525 (Co)	2.21	2.62	1.1	1.87	16
NUM-9	2.47	2.36	1.61	1.45	17
NUM-9※	2.9	2.95	1.85	1.52	17
NPU-1	4.50	5.09	1.32	1.4	18
NPU-2	4.42	4.02	1.52	1.25	18
NPU-3	3.33	2.54	3.2	1.3	18
UiO-67	3.05	2.09	1.49	1.07*	19
UiO-67-$(NH_2)_2$	5.32	5.9	1.7	2.1*	19
Zn-atz-ipa	1.81	1.99	1.7	--	20
Zn-atz-oba	2.05	2.77	1.27	1.43	21

※: At 1 bar and 273 K temperature; ‡: At 1 bar and 303 K temperature; *: IAST selectivity for 1/99 gas mixture;

Reference

1. W. Liang, T. L. Church, S. Zheng, C. Zhou, B. S. Haynes and D. M. D'Alessandro, *Chem. Eur. J.*, 2015, **21**, 18576-18579.
2. Z. Chen, S. Xiang, T. Liao, Y. Yang, Y.-S. Chen, Y. Zhou, D. Zhao and B. Chen, *Cryst. Growth Des.*, 2010, **10**, 2775-2779.
3. C.-Y. Chen, H.-C. Lu, C.-G. Wu, J.-G. Chen and K.-C. Ho, *Adv. Funct. Mater.*, 2007, **17**, 29-36.

4. J. VandeVondele, M. Krack, F. Mohamed, M. Parrinello, T. Chassaing and J. Hutter, *Comput. Phys. Commun.*, 2005, **167**, 103-128.
5. S. Goedecker, M. Teter and J. Hutter, *Phys. Rev. B*, 1996, **54**, 1703-1710.
6. C. Hartwigsen, S. Goedecker and J. Hutter, *Phys. Rev. B*, 1998, **58**, 3641-3662.
7. M. Krack and M. Parrinello, *Phys. Chem. Chem. Phys.*, 2000, **2**, 2105-2112.
8. J. VandeVondele and J. Hutter, *J. Chem. Phys.*, 2007, **127**, 114105.
9. J. P. Perdew, K. Burke and M. Ernzerhof, *Phys. Rev. Lett.*, 1996, **77**, 3865.
10. S. Grimme, J. Antony, S. Ehrlich and H. Krieg, *J. Chem. Phys.*, 2010, **132**, 154104.
11. H.-G. Hao, Y.-F. Zhao, D.-M. Chen, J.-M. Yu, K. Tan, S. Ma, Y. Chabal, Z.-M. Zhang, J. M. Dou, Z.-H. Xiao, G. Day, H.-C. Zhou and T. B. Lu, *Angew. Chem. Int. Ed.*, 2018, **57**, 16067-16071.
12. Z. Xu, X. Xiong, J. Xiong, R. Krishna, L. Li, Y. Fan, F. Luo and B. Chen, *Nat. Commun.*, 2020, **11**, 3163.
13. L. Fan, P. Zhou, X. Wang, L. Yue, L. Li and Y. He, *Inorg. Chem.*, 2021, **60**, 10819-10829.
14. Z. Jiang, L. Fan, P. Zhou, T. Xu, S. Hu, J. Chen, D.-L. Chen and Y. He, *Inorg. Chem. Front.*, 2021, **8**, 1243-1252.
15. R. E. Sikma, N. Katyal, S. K. Lee, J. W. Fryer, C. G. Romero, S. K. Emslie, E. L. Taylor, V. M. Lynch, J. S. Chang, G. Henkelman and S. M. Humphrey, *J. Am. Chem. Soc.*, 2021, **143**, 13710-13720.
16. Y. Wang, C. Hao, W. Fan, M. Fu, X. Wang, Z. Wang, L. Zhu, Y. Li, X. Lu, F. Dai, Z. Kang, R. Wang, W. Guo, S. Hu and D. Sun, *Angew. Chem. Int. Ed.*, 2021, **60**, 11350.
17. S.-Q. Yang, F.-Z. Sun, P. Liu, L. Li, R. Krishna, Y.-H. Zhang, Q. Li, L. Zhou and T.-L. Hu, *ACS Appl. Mater. Interfaces*, 2021, **13**, 962-969.
18. B. Zhu, J.-W. Cao, S. Mukherjee, T. Pham, T. Zhang, T. Wang, X. Jiang, K. A. Forrest, M. J. Zaworotko and K.-J. Chen, *J. Am. Chem. Soc.*, 2021, **143**, 1485-1492.
19. X.-W. Gu, J.-X. Wang, E. Wu, H. Wu, W. Zhou, G. Qian, B. Chen and B. Li, *J. Am. Chem. Soc.*, 2022, **144**, 2614-2623.
20. K.-J. Chen, D. G. Madden, S. Mukherjee, T. Pham, K. A. Forrest, A. Kumar, B. Space, J. Kong, Q.-Y. Zhang, M. J. Zaworotko, *Science*, 2019, **366**, 241-246.
21. J.-W. Cao, S. Mukherjee, T. Pham, Y. Wang, T. Wang, T. Zhang, X. Jiang, H. J. Tang, K. A. Forrest, B. Space, M. J. Zaworotko and K. J. Chen, *Nat. Commun.*, 2021, **12**, 6507.